A Study on Interface Healing in Polypropylene Processing

Gregory D. Smith, Staffan Toll and Jan-Anders E. Månson*

Laboratoire de Technologie des Composites et Polymères
Ecole Polytechnique Fédérale de Lausanne
CH-1015 Lausanne, Switzerland

Introduction

Examples of interface healing are the impingement of two melt fronts during injection molding or during extrusion of hollow sections and the fusion of thin films during heat sealing. A different case is the wetting of a solid polymer by a molten one to form a bond by fusion. This latter situation arises in the integration of subcomponents as polymeric inserts in injection or compression molding. We are currently developing such techniques for the production of structural components that use advanced thermoplastic composites for mechanical performance and engineering plastics for complex shape. In a recent communication [1] we examined the potential economic and performance advantages of such an integrated processing approach. However, these advantages can only be achieved if the bond between sub-components is sufficiently strong and reliable.

The study of interface healing was initially focussed on amorphous polymers [2,3]; but currently addresses the more complicated healing processes of semi-crystalline polymers [4,5]. A key requirement for the investigation of healing in polymer processing is precise control over the processing parameters, e.g., temperature and pressure. An often used technique for weld-line studies is dual gate injection molding [4,6]. This method can define the processing window for acceptable bond strengths in terms of the injection parameters: melt temperature, mold temperature and injection pressure, but it is difficult to relate these values to the conditions at the impinging melt fronts. The melt temperature at a flow front is especially difficult to control due to viscous heating and heating by compression of air in the cavity. In this work we present an experimental technique which involves a minimum of flow and allows correspondingly better, and separate, control of temperature and pressure.

Experimental

The material used in this work is a controlled rheology grade polypropylene (VM6100H) manufactured by Shell Chemicals. This is an injection molding grade with a low and narrow molecular weight distribution. Plaques for the bonding experiments, 50 mm by 50 mm by approximately 2 mm thick, were injection molded on a Butler 10/90 HI-TECH injection molding unit. The melt injection temperature was 195°C and the injection pressure was 60 MPa for the injection phase and 20 MPa for the holding phase. The mold temperature was 100°C.

The bonding experiments were conducted using an instrumented matched-die mold. This mold was designed to achieve close temperature control of the upper and lower mold halves independently. A schematic of the mold with the heating and cooling systems is shown in Figure 1. The temperature is recorded as a function of time via thermocouples located at the

* To whom correspondence should be addressed

upper and lower mold faces. The mold was installed on a servo-hydraulic load frame. A plaque was attached to each mold half and allowed to equilibrate at temperature for 10 minutes. Bonds were made by bringing both plaques, either at the same or at different initial temperatures, into contact by closing the mold to a pressure of 2 MPa for a specified hold time, at which point the heating was turned off and the cooling initiated. The pressure was maintained until the mold reached room temperature.

Two test series were conducted. The first series was isothermal. The upper and lower mold halves were heated to the same temperature (±1°C) between 150 to 180°C. The hold time was 10 minutes. The second series was non-isothermal. The lower mold was kept constant at 200°C while the temperature of the upper mold was varied between 100 to 160°C. The hold time was 42 seconds.

Fracture specimens, 10 mm by 50 mm were cut from the bonded specimens. A starter crack was initiated by aligning a single edged razor blade with the plane of the interface and pressed down until a crack formed at the interface. The initial crack length was approximately 10 mm. The fracture energy of the bonds was measured using a double cantilever beam geometry with a constant crack opening displacement as shown in Figure 2. Crack propagation was accomplished by forcing the specimens over the razor blade in a screw driven load frame at a crosshead speed of 2 mm/minute. Usually, the crack front was quite stable during propagation, but did vary somewhat with position. Occasionally the crack front would reach an area of poor bonding and jump 2 to 3 mm, stopping at the next area of higher toughness and grow as before. Only data from areas of stable crack growth have been reported. The crack area was illuminated by placing a lamp behind the specimens and recording the crack area as a function of position using a video camera. Afterwards, the video images were captured and digitized on a personal computer using image analysis software. The area of the crack surface was measured at 2.5 mm intervals over a 10 mm section at the mid-point of the specimen. The crack length was calculated by dividing the measured area by the local width of the specimen.

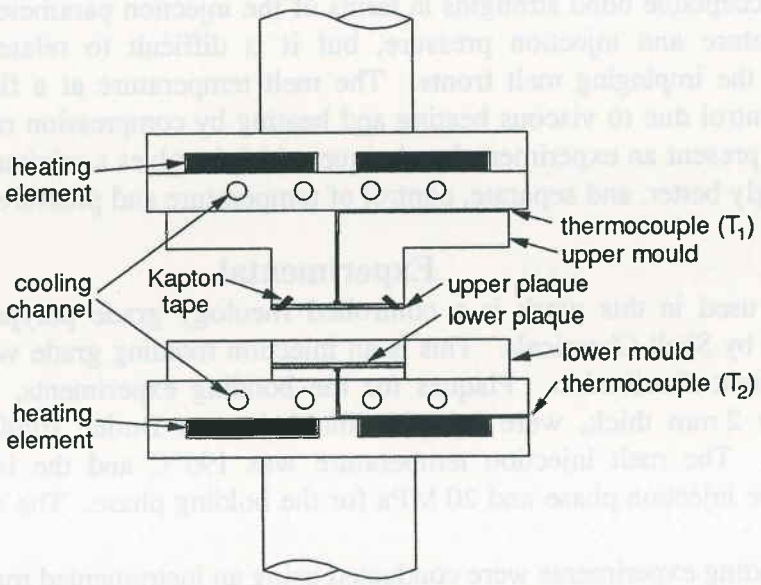

Figure 1: Schematic of the instrumented matched mold showing the heating elements, cooling channels, position of sample plaques and the method of attachment of the upper plaque to the upper mold.

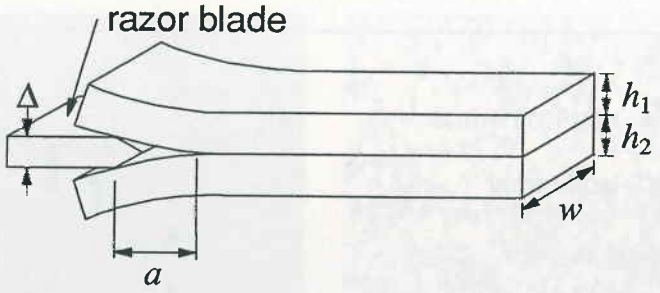

Figure 2: Schematic of the fracture geometry used to measure the critical strain energy release rate. A double cantilever beam test with a constant crack opening displacement.

Optical microscopy was used to characterize the fracture surfaces and cross-sectional morphology of the interface. The fracture surfaces were studied using illumination at a shallow angle, approximately 5° from the horizontal, to emphasize the surface texture. The morphology was studied on microtomed sections, (approximately 10 μm thick) cut perpendicular to the interface plane, viewed between crossed polarizers.

Results

The critical strain energy release rate was calculated using an equation derived by Kanninen [7] based on simple beam bending. Assuming that all the elastic energy released upon fracture is absorbed by the plastic deformation at the crack tip, a simple approximation for the released elastic energy can be obtained assuming that the only contribution to the elastic energy is the bending of each beam and that no energy is stored ahead of the crack tip [8]. In this case G_c, is given by

$$G_c = \frac{3\Delta^2 E h_1 h_2}{8a^4(h_1^3 + h_2^3)}$$

where Δ is the wedge thickness, E is the elastic modulus, h_1 and h_2 are the beam thicknesses, a is the crack length and w is the width.

The interface temperature is here described by the average temperature of the two plaques before they are brought into contact,

$$\overline{T} = ½(T_1 + T_2).$$

For the isothermal experiments this is certainly correct; the temperature difference between the upper and lower plaques was less than 2°C. For the non-isothermal experiments, it is correct immediately after contact, before any melting or crystallization has taken place.

The fracture energies for both series as functions of the average temperature are shown in Figure 3. The overall trend is increasing fracture energy with temperature. At low temperatures there is very little bonding with the fracture energy increasing only slightly as the melting temperature is approached. However, once the melting temperature is exceeded, the fracture energy increases rapidly for the non-isothermal series, and gradually for the isothermal series.

There are essentially 3 different ranges of bond strengths: (1) low fracture energy bonds made below the melting point, (2) bonds made above the melting point with intermediate values of fracture energy, and (3) bonds with high values of fracture energy made well above

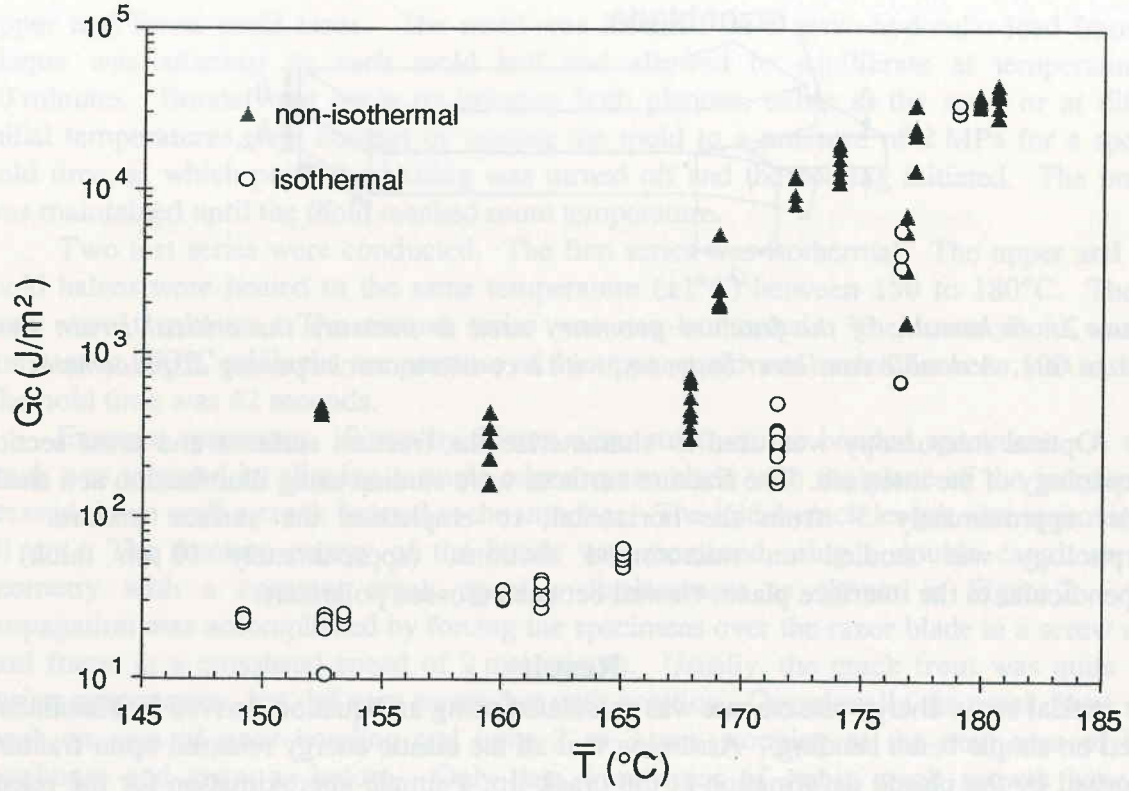

Figure 3: The critical strain energy release rate as a function of average initial plaque temperature for the isothermal case.

the melting point. Investigation of the fracture surface and morphology will elucidate the bonding process.

The surface texture of an as-molded plaque is shown in Figure 4a. The striation pattern is due to the melt taking on the surface texture of the mold during injection molding (a ground surface in this case). The morphology of a plaque before bonding is shown in cross-section in Figure 4b. The skin-core morphology, which is well known in injection molding [9], is clearly seen. The dark region just above the plaque surface is a shear zone. It is produced by shear between the less viscous melt at the center of the plaque and the cooler, more viscous, material adjacent to the mold wall. Closer examination of the shear zone reveals that it is composed of row nucleated crystalline clusters as reported by [10]. Elongation of the polymer molecules in these zones was confirmed by placing a plaque on a hot plate. As the plaque melts it pulls back from the edges and the thickness increases over time. This orientation effect is more pronounced towards the gate than at the closed end of the mold. This effect is particularly important since elongated chains have a higher local melting temperature than the bulk material [11], thus once produced, slightly higher temperatures are required to erase them.

The fracture surfaces of an isothermal and a non-isothermal bond made below the melting point, at 160°C, are shown in Figure 5a and b. For the isothermal bond there is very little change in its surface texture. Since we are 5°C below the measured melting point (165.2°C peak temperature via DSC) the material is essentially solid, and the absence of any significant bonding is as expected. The cross-sections of these bonds are shown in Figure 5c and d. For the isothermal bond, the original morphology is essentially preserved. For the upper plaque of the non-isothermal bond, the temperature never exceeds the melting point, and the original morphology is also preserved. However, the morphology of the lower plaque, which was initially molten, is considerably different. The cooling rate for the bonding process is much lower than during the injection molding process and produces correspondingly larger

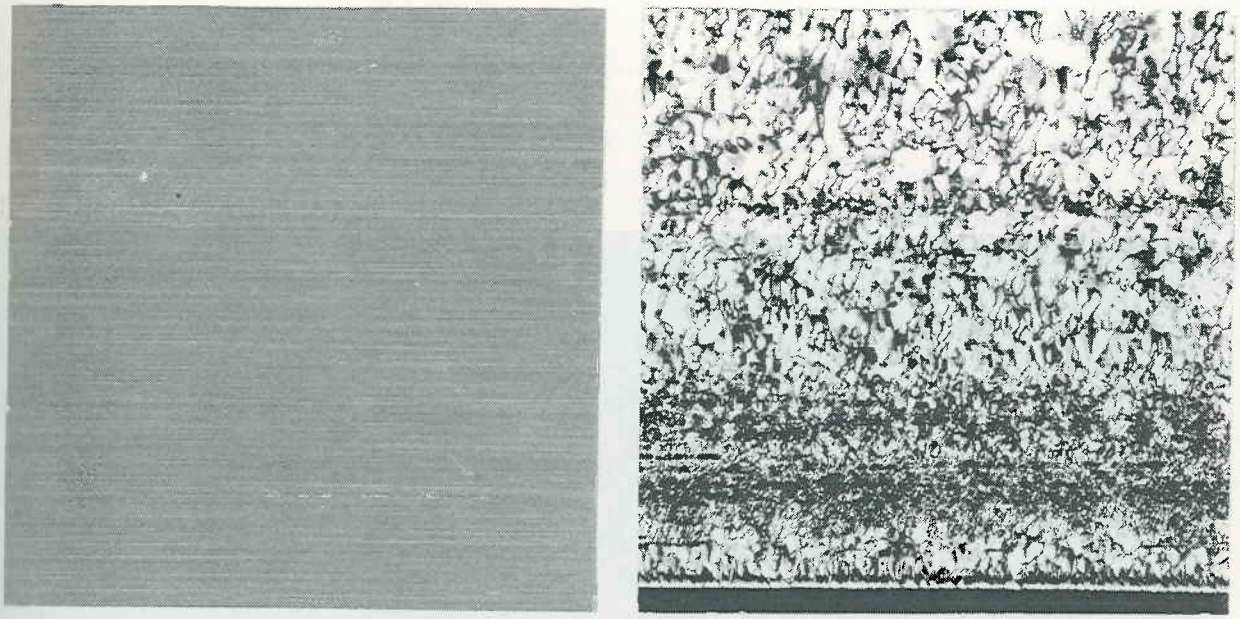

Figure 4: The surface and cross-sectional morphology of an as-molded plaque. (a) Surface morphology, note the striation pattern due to the ground surface of the mold; (b) Cross-sectional morphology midway along the centerline.

spherulites. The area directly adjacent to the interface in the lower plaque is a transcrystalline α-phase. Slightly below the interface an occasional β-phase spherulite (the white cone shaped areas) can be seen. The existence of the β-phase was confirmed by heating a microtomed section above the melting temperature of the β-phase, 152°C [10], where they were observed to first turn dark, exhibiting no birefingence, and then recrystallize into the α-phase. This phenomenon has been reported by Varga [12]. The β-phase has a higher growth rate than the α-form; thus, once the β-phase has nucleated, it grows radially and overtakes the α-phase growing beside it and produces cone-shaped spherulites.

The fracture surfaces of the bonds made slightly above the melting point, approximately 5°C, are shown in Figure 6a and b. The original texture is still very apparent for the isothermal bond, again indicating that little melting took place. The white areas on the tops of the striations are likely due to plastic deformation during crack growth. The absence of any texture between the striations suggests that intimate contact was not obtained over the whole interfacial area. The original surface texture is completely erased for the non-isothermal bond, suggesting that the surface did indeed melt. This bond has a fracture energy which is approximately an order of magnitude higher than the isothermal bond. The white areas perpendicular to the crack propagation direction are cracks which grow down into the plaque in the direction of crack propagation. Thus this bond has an additional means of dissipating energy which is not available in the isothermal case. The cross-sections for these bonds are shown in Figure 6c and d. The morphology of the plaques is generally the same as for the bonds made below the melting point, with one important difference. Examining the area directly above the interface, one can see that the original columnar morphology in this region has been tilted, indicating that this layer was molten and subjected to some amount of shear (cf. [13]). Although not evident in the micrograph, the frequency of the cone-shaped β-phase spherulites is approximately the same as in Figure 5d when examined over a longer portion of interface.

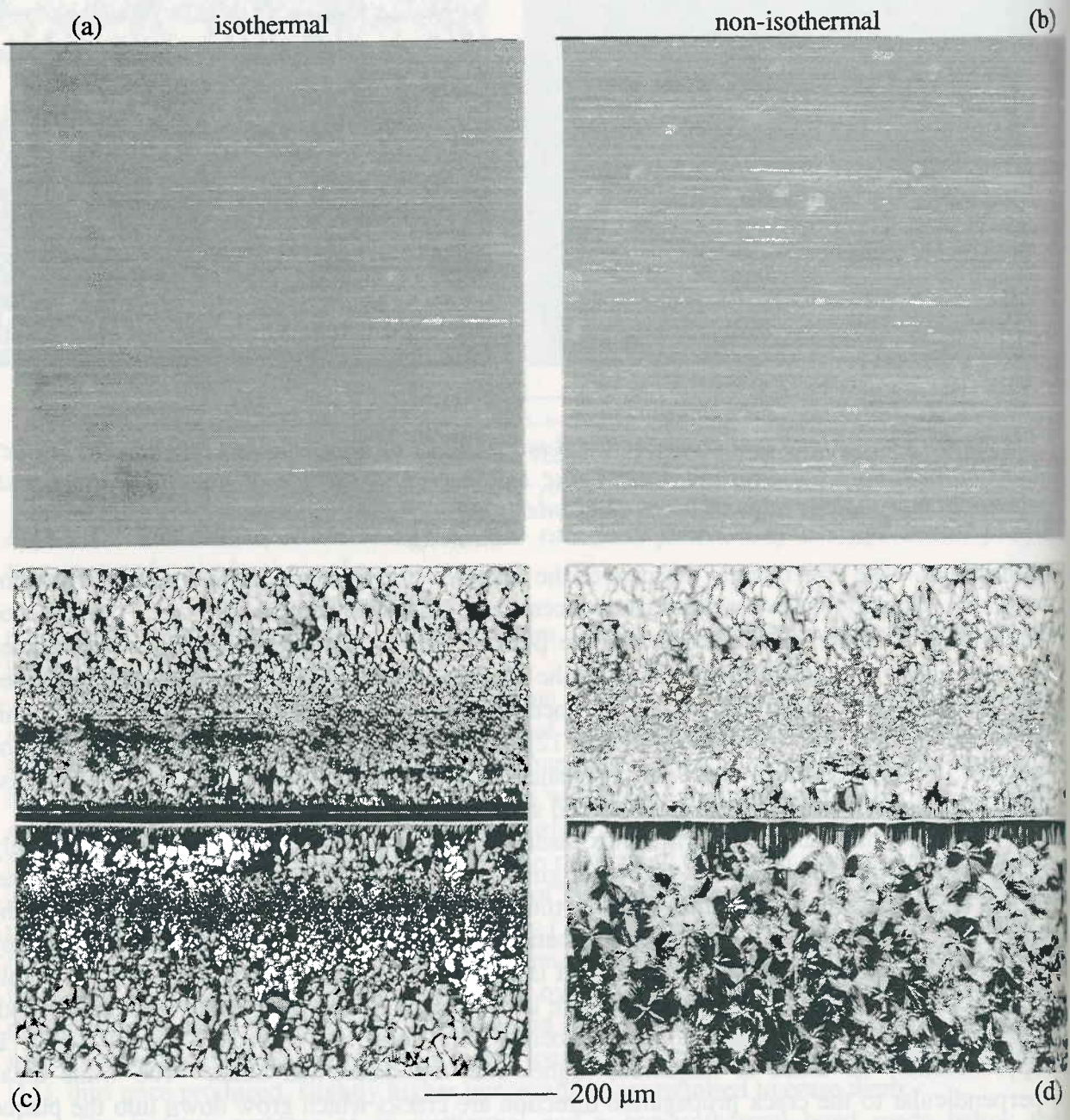

Figure 5: The fracture surfaces (a) and (b) and cross-sectional morphologies (c) and (d) for the bonds made at 160°C. Crack propagation was from left to right for all micrographs.

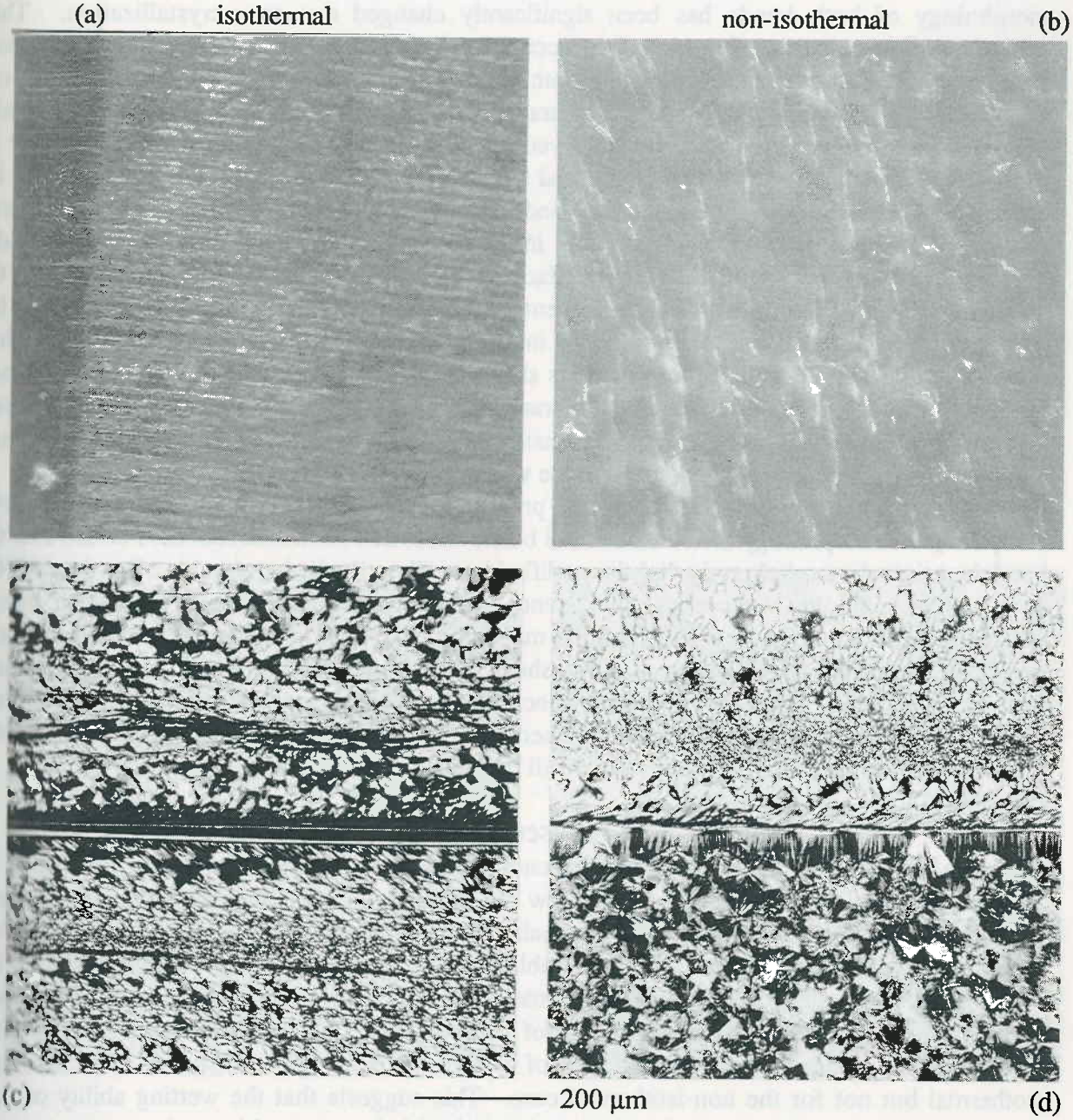

Figure 6: The fracture surfaces (a) and (b) and cross-sectional morphologies (c) and (d) for the bonds made at 170°C. The dark region to the left of a is due to the edge of the razor blade flattening the fracture surface.

The fracture surfaces for bonds made at 180°C are shown in Figure 7a and b. At this temperature the original surface texture of the isothermal bond has been completely erased. The overall appearance of the fracture surfaces are similar but the non-isothermal bond has a more uniform, finer, texture and is likely the reason for its slightly higher fracture energy compared to the isothermal case. The cross-sections are shown in Figure 7c and d. The morphology of both bonds has been significantly changed due to recrystallization. The occasional disappearance of the interface occurs for both types of bonds. For the isothermal bond, a transcrystalline phase grows into both plaques and the spherulite size on either side of the interface is essentially the same. The transcrystalline zone was only present for a small fraction of the length of the interface observed for the isothermal bond but was present over a much large fraction for the non-isothermal bond. The structure of the lower plaque is essentially the same for the isothermal and non-isothermal bonds. The spherulites are somewhat smaller in the upper plaque than in the lower plaque for the non-isothermal bond. The maximum temperature of the top surface of this plaque was measured to be 169.5°C indicating that the whole plaque underwent melting, and explains the drastic change in morphology from the initial state. Also of interest is the plane of crack propagation for the non-isothermal bond. The fracture plane is shifted back and forth between the interface and the region just below the interface in the α-transcrystalline zone. Failure in the transcrystalline layer has been observed by Gehde and Ehrenstein [14] for extrusion welded polypropylene and could be significant since it may represent the weakest link in a bond.

Some insight into the recrystallization process for the isothermal series can be gained by comparing the morphology of the isothermal bonds made at 170°C and 180°C. For the 170°C bond the original morphology is slightly modified but still easily distinguishable. For the 180°C bond the morphology is completely different. An intermediate morphology between these extremes is shown in Figure 8 for the bond made at 176.6°C. The spherulites are much finer here than in the unbonded plaque and the shear zone has disappeared. In the upper plaque there is a dark zone. Since it is in the same location as the shear zone we can conclude that the shear zone has recrystallized into small spherulites [10,14]. Moving into the bulk of either plaque, traces of the original structure can still be seen.

Discussion

Generally, the relationship between fracture energy and average temperature shown in Figure 3 is what one would intuitively expect. Below the melting temperature minimal bonding takes place due to the inhibition of the polymer chains by the crystalline domains. Once the melting temperature is exceeded, there is a considerable increase in the molecular mobility, resulting in higher bond strengths for the same hold time. At sufficiently high temperatures, the bond strength approaches the cohesive strength of the bulk material, and levels out. Below the melting point a temperature dependence of the fracture energies seems to exist for the isothermal but not for the non-isothermal case. This suggests that the wetting ability of the melt is solely responsible for the bond strengths attained below the melting point.

It is interesting that in both experimental series some degree of bonding, albeit very small, was obtained for average temperatures below the peak melting temperature. A possible explanation may be the kind of auto-adhesion observed for rubbers [15]. The melting range for semi-crystalline polymers can be quite wide and partial melting takes place below the peak melting temperature. In this range the material will be very flexible and behave much like a rubber, thereby allowing intimate contact. In addition, there may be some limited interpenetration of the molecular chains in the molten regions.

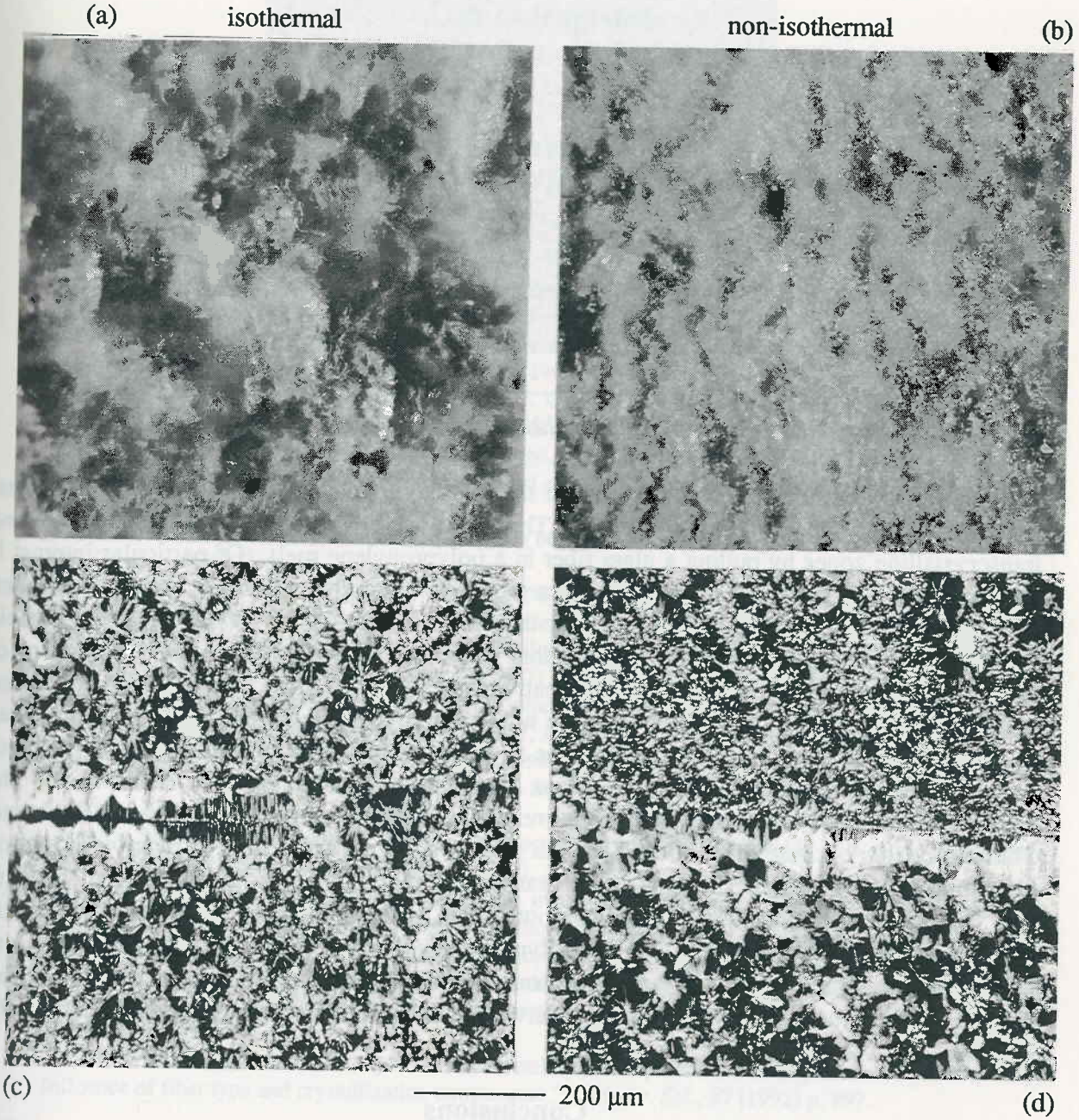

Figure 7: The fracture surfaces (a) and (b) and cross-sectional morphologies (c) and (d) for the bonds made at 180°C.

Figure 8: The morphology of an isothermal bond made at 176.6°C.

A transcrystalline zone occurs in all of the non-isothermal bonds and only at the highest temperature for the isothermal bonds. Thomason and Van Rooyen [16,17] produced transcrystalline zones by pulling a glass fiber in a polypropylene melt. Of particular interest is the formation of a transcrystalline zone in a region where the glass fiber was completely pulled out of the melt, suggesting that shear, rather than the presence of the glass fiber, is responsible for the transcrystalline zone. They propose that the shear stress produces extended portions of the polymer chains which act as nucleation sites. This may explain the observed transcrystalline zones in this work. For the non-isothermal experiments, nucleation sites may be present on the surface of the plaques due to shear during injection molding, and produces the transcrystalline zone that grows into the lower, molten, plaque. However, the transcrystalline zone never grows into the melted layer of the upper, originally solid, plaque. This is probably because this region is molten for too short a time to lose its previous structure [10] thus suppressing the formation of a transcrystalline zone. For the isothermal bond at 180°C, a transcrystalline zone develops on both sides of the interface. Since both plaques are well above the melting temperature, the polymer chains are much more mobile and thus lose their previous structure. During cooling, some extended chains remain, due to their higher melting temperature, and produce the observed transcrystalline zones on both sides of the interface.

Conclusions

1. The presented technique using an instrumented matched-die mold allows melt interface healing to be studied with close control over the process parameters, e.g., temperature and pressure.
2. At a given interface temperature below the melting point of the polymer, much higher G_c is obtained non-isothermally, i.e., when one of the adherends is molten, than isothermally. This is most likely due to the intimate contact achieved through wetting.
3. The bond strength increases monotonically with interface temperature with a transition around the melting temperature of the polymer.

4. Non-isothermal bonding generally gives a stronger bond than isothermal bonding, although the difference appears to diminish towards high interface temperatures.
5. The frozen-in orientation of the polymer chains is probably the nucleation mechanism which produces the α-phase transcrystalline zone.

Acknowledgement

We would like to acknowledge the Priority Program for Materials (PPM) in Switzerland for their financial support of this work.

References

1. Smith, G.D., S. Toll and J.-A. E. Månson, "Integrated processing of multi-functional composite structures," 39th Int. SAMPE Symp. (1994) p. 2385.
2. Wool, R.P. and K.M. O'Connor, "A theory of crack healing in polymers," *J. Appl. Phys.*, **52** (1981) p. 5953.
3. Jud, K., H.H. Kausch and J.G. Williams, "Fracture mechanics studies of crack healing and welding of polymers," *J. Mater. Sci.*, **16** (1981) p. 204.
4. Nadkarni, V.M. and S.R. Ayodhya, "The influence of knit-lines on the tensile properties of fiberglass reinforced thermoplastics," *Polym. Eng . Sci.*, **33** (1993) p. 358.
5. Aboulfaraj, M., M. Coquebert de Neuville and C. G'Sell, "Influence of temperature and pressure on the structure and strength of polypropylene weld joints," Deformation, Yield and Fracture of Polymers, The Institute of Materials, Churchill College, Cambridge, U.K. (1994) p. P46/1.
6. Gardner, G. and C. Cross, "The effect of a heated core-pin on the weld strength of polypropylene," *SPE ANTEC Technical Papers*, **38** (1992) p. 2127.
7. Kanninen M. F., "An augmented double cantilever beam model for studying crack propagation and arrest," *Int. J. Fract.*, **9** (1973) p. 83.
8. Creton C., E.J. Kramer, Hui, C.-Y. and H.R. Brown, "Failure Mechanisms of Polymer Interfaces Reinforced with Block Copolymers," *Macromolecules*, **25** (1992) p. 3075.
9. Karger-Kocsis, J., "Skin-core morphology and failure of injection-molded specimens of impact modified polypropylene blends," *Polym. Eng . Sci.*, **27** (1987) p. 4.
10. Varga, J., "Review-Supermolecular structure of isotactic polypropylene," *J. Mater. Sci.*, **27** (1992) p. 2557.
11. Wunderlich, B. *Macromolecular Physics Volume 2*, Academic Press, New York (1976) p. 66.
12. Varga, J. and J. Karger-Kocsis, "The occurrence of transcrystalline or row-nucleated cylindritic crystallization as a result of shearing in a glass-fiber-reinforced polypropylene," *Comp. Sci. Tech.*, **48** (1993) p. 191.
13. Oliveira, M.J. and D.A. Hemsley, "The microstructure of polypropylene welds as a guide to processing history," *British Polymer Journal*, **17** (1985) p. 269.
14. Gehde M. and G.W. Ehrenstein, "Structure and mechanical properties of optimized extrusion welds," Advances in Joining Plastics and Composites, Bradford, Yorkshire UK, 1991, p. 236
15. Kausch, H.H. and M. Tirrell, "Polymer Interdiffusion," *Annu. Rev. Mater. Sci.*, **19** (1989) p. 341.
16. Thomason J.L. and A.A. Van Rooyen, "Transcrystallized interphase in thermoplastic composites, Part 1, Influence of interfacial stress, cooling rate, fibre properties and polymer molecular weight," *J. Mater. Sci.*, **27** (1992) p. 889.
17. Thomason J.L. and A.A. Van Rooyen, "Transcrystallized interphase in thermoplastic composites, Part 2, Influence of fiber type and crystallization temperature," *J. Mater. Sci.*, **27** (1992) p. 897.